

Synthesis and Structure of Coordination Polymers of Ag(I) with Isomeric (Aminomethyl)pyridines. Formation of A Novel Circular Helicate and 2-D Networks via Ag...Ag Contacts and Coordination Shell Expansion under Anion Control

S. Sailaja and M. V. Rajasekharan*

School of Chemistry, University of Hyderabad, Hyderabad 500 046, India

Received March 2, 2003

Reaction between Ag(I) salts and the three isomers of (aminomethyl)pyridines, viz., 2-amp, 3-amp, and 4-amp, lead to either discrete or polymeric (1-D and 2-D) structures influenced by anions and closed shell Ag...Ag contacts. Characterization data for Ag(2-amp)BF₄ (**1**) follow: monoclinic, space group *C2/c*, with $a = 16.788(2)$ Å, $b = 11.5719(6)$ Å, $c = 11.3864(7)$ Å, $\beta = 123.671(8)^\circ$, and $Z = 8$. For Ag₂(2-amp)₃(PF₆)₂ (**2**): monoclinic, space group *P2₁/a*, with $a = 10.029(7)$ Å, $b = 20.291(12)$ Å, $c = 13.907(6)$ Å, $\beta = 95.38(5)^\circ$, and $Z = 4$. For Ag₂(3-amp)₃(PF₆)₂ (**4**): triclinic, space group *P $\bar{1}$* , with $a = 10.4482(7)$ Å, $b = 11.1468(9)$ Å, $c = 12.2720(11)$ Å, $\alpha = 81.018(7)^\circ$, $\beta = 80.668(6)^\circ$, $\gamma = 80.977(6)^\circ$, and $Z = 2$. For Ag(4-amp)BF₄·0.75CH₃CN (**5**): orthorhombic, space group *C22₂₁*, with $a = 9.272(2)$ Å, $b = 16.164(12)$ Å, $c = 27.851(2)$ Å, and $Z = 8$. For Ag(4-amp)PF₆ (**6**): monoclinic, space group *P2₁/m*, with $a = 5.2089(7)$ Å, $b = 14.3950(17)$ Å, $c = 7.0149(14)$ Å, $\beta = 96.538(14)^\circ$, and $Z = 2$. While Ag(I) is 2-coordinate in **1**, **5** and **6**, it shows 3-coordination in **2** and **4**. Compound **1** consists of a 1-D polymeric cation chain with interchain Ag...Ag contacts and the anions sitting on the edges of the chains. The dication in **2** is held in the form of a circular helicate by closed shell Ag...Ag interactions. Compound **4** generates a 2-D network with channels big enough to accommodate the anions. Compound **5** is a 2-D chiral network of chains connected by Ag...Ag contacts. Compound **6** shows a simple 1-D chain structure with an alternating arrangement of cationic chains and anions.

Introduction

Ag⁺ ion forms numerous one-dimensional coordination polymers with bridging ligands. While the main reason behind this tendency is the general preference of this ion for linear 2-coordination, the structure and packing of the chains are often greatly influenced by Ag...Ag closed shell interaction as well as counterions present in the crystal. Quite often, the coordination number may increase to 3, 4, and even up to 6, leading to higher dimensional networks. Recently reported silver coordination polymers include helical chains capable of exchanging the anions held in the chiral tunnels with those in solution,¹ triple helical chains,² ladders,³ stairs,⁴ wafers⁵ (5- and 6-coordination), lamellar⁶ and microporous⁷ networks, wavelike⁸ and T-shaped⁹ archi-

tectures, and diamondoid¹⁰ structures. The role of anions in controlling the network formation has been noted in several cases.^{6,10,11} We have recently reported the ClO₄⁻ salts of Ag-(I) polymers with the three isomeric (aminomethyl)pyridines.² The present study shows that BF₄⁻ and PF₆⁻ anions lead to very different and novel structures. Within this simple

* To whom correspondence should be addressed. E-mail: mvrsc@uohyd.ernet.in.

(1) Jung, O.-S.; Kim, Y. J.; Lee, Y.-A.; Chae, H. K.; Jang, H. G.; Hong, J. *Inorg. Chem.* **2001**, *40*, 2105.

(2) Sailaja, S.; Rajasekharan, M. V. *Inorg. Chem.* **2000**, *39*, 4586.

(3) Kang, Y.; Lee, S. S.; Park, K.-M.; Lee, S. H.; Kang, S. O.; Ko, J. *Inorg. Chem.* **2001**, *40*, 7027.

(4) Zhang, L.; Cheng, P.; Tang, L.-F.; Weng, L.-H.; Jiang, Z.-H.; Liao, D.-Z.; Yan, S.-P.; Wang, G.-L. *Chem. Commun.* **2000**, 717.

(5) Carlucci, L.; Ciani, G.; Proserpio, D. M.; Sironi, A. *Angew. Chem., Int. Ed. Engl.* **1995**, *34*, 1895.

(6) Hong, M.; Su, W.; Cao, R.; Fujita, M.; Lu, J. *Chem. Eur. J.* **2000**, *6*, 427.

(7) Zheng, S.-L.; Tong, M.-L.; Fu, R.-W.; Chen, X.-M.; Ng, S.-W. *Inorg. Chem.* **2001**, *40*, 3562.

(8) Carlucci, L.; Ciani, G.; Gudenberg, D. W. v.; Proserpio, D. M. *Inorg. Chem.* **1997**, *36*, 3812.

(9) Robinson, F.; Zaworotko, M. J. *J. Chem. Soc., Chem. Commun.* **1995**, 2413. Yaghi, O. M.; Li, H. *J. Am. Chem. Soc.* **1996**, *118*, 295.

(10) Hirsch, K. A.; Wilson, S. R.; Moore, J. S. *Chem. Eur. J.* **1997**, *3*, 765.

isomeric group of bidentate ligands, the anions influence the stoichiometry, packing, and dimensionality (0, 1, 2) of the Ag(I) complexes.

Experimental Section

Synthesis. AgBF₄ and AgPF₆ were purchased from Acros Chemicals. The compounds 2-amp, 3-amp, and 4-amp were purchased from Lancaster Chemicals. In all cases, white precipitates were obtained by adding an equimolar amount of ligand to the silver(I) salt dissolved in about 10 mL of water, and stirring for about 15–20 min at room temperature. The precipitate was filtered, washed with cold water, and dried. Crystals for X-ray analysis were obtained by slow evaporation of an aqueous solution over conc H₂SO₄ in a desiccator or from acetonitrile at room temperature. The amount of reagents used, yield, and analytical data are mentioned under individual compounds in the following paragraphs. In three cases, the initial precipitate and crystals had different compositions. In such cases, C, H, N data are quoted for both samples.

Ag(2-amp)BF₄ (1). This reaction used 2-amp, 0.65 mL (6.3 mmol), and AgBF₄, 1.283 g (6.59 mmol), to yield 1.520 g (5.02 mmol, 79%). Colorless, block shaped crystals (from water) formed. Anal. Calcd for C₆H₈N₂F₄BAG: C, 23.80; H, 2.66; N, 9.25. Found: C, 23.77; H, 3.10; N, 8.61. Characteristic IR peaks (cm⁻¹): 3345, 1595, 1478, 1437, 1304, 1057(b), 762, 611.

Ag₂(2-amp)₃(PF₆)₂ (2). This reaction required 2-amp, 0.20 mL (1.9 mmol), and AgPF₆, 0.513 g (2.03 mmol), to yield 0.560 g (1.55 mmol, 80%) of Ag(2-amp)PF₆. Anal. Calcd for C₆H₈N₂F₆PAG: C, 19.96; H, 2.23; N, 7.76. Found: C, 19.66; H, 2.49; N, 7.41. Colorless block shaped crystals of **2** (from water) formed. Anal. Calcd for C₁₈H₂₄N₆F₁₂P₂Ag₂: C, 26.05; H, 2.91; N, 10.12. Found: C, 26.26; H, 2.55; N, 9.86. Characteristic IR peaks (cm⁻¹): 3341, 1595, 1478, 1437, 1150, 841, 611, 559. NMR chemical shifts (δ/ppm) in CH₃CN-*d*₃, with values for the free ligand given within brackets) ¹H: amino, 2.10 (1.94); methylene, 4.20 (4.00); pyridyl 5H, 7.50 (7.32); 3H, 7.50 (7.49); 4H, 7.99 (7.83); 6H, 8.63 (8.63). ¹³C: methylene, 47.01 (48.45); pyridyl 5C, 124.15 (121.72); 3C, 124.49 (122.38); 4C, 139.04 (137.24); 6C, 150.88 (149.80); 2C, 159.85 (163.87).

Ag(3-amp)BF₄ (3). This reaction used 3-amp, 0.52 mL (5.1 mmol), and AgBF₄, 1.071 g (5.50 mmol), to yield 0.857 g (2.83 mmol, 55%). Colorless, block shaped crystals (from water) formed. The crystals lose crystallinity slowly and turn to a pink color. Anal. Calcd for C₆H₈N₂F₄BAG: C, 23.80; H, 2.66; N, 9.25. Found: C, 24.03; H, 2.60; N, 8.69. Due to poor quality of the crystals, single-crystal X-ray data could not be collected. Characteristic IR peaks (cm⁻¹): 3360, 1595, 1481, 1431, 1300, 1057(b), 790, 710, 639, 520.

Ag₂(3-amp)₃(PF₆)₂ (4). This synthesis used 3-amp, 0.11 mL (1.1 mmol), and AgPF₆, 0.254 g (1.00 mmol), to yield 0.260 g (0.72 mmol, 72%) of Ag(3-amp)PF₆. Anal. Calcd for C₆H₈N₂F₆PAG: C, 19.96; H, 2.23; N, 7.76. Found: C, 20.74; H, 1.73; N, 7.86. Colorless block shaped crystals of **4** (from water) formed. Anal. Calcd for C₁₈H₂₄N₆F₁₂P₂Ag₂: C, 26.05; H, 2.91; N, 10.12. Found:

C, 26.07; H, 2.74; N, 9.46. Characteristic IR peaks (cm⁻¹): 3414, 1615, 1483, 1431, 1397, 831, 710, 640, 559.

Ag(4-amp)BF₄·0.75CH₃CN (5). This reaction required 4-amp, 0.50 mL (4.9 mmol), and AgBF₄, 1.010 g (5.19 mmol), to yield 1.46 g (4.82 mmol, 98%) of Ag(4-amp)BF₄. Colorless block shaped crystals (from acetonitrile) formed. Anal. Calcd for C_{7.5}H_{10.25}N_{2.75}F₄-BAG: C, 27.00; H, 3.10; N, 11.55. Found: C, 27.09; H, 3.05; N, 11.50. Characteristic IR peaks (cm⁻¹): 3337, 1609, 1562, 1429, 1360, 1057, 926, 795, 631.

Ag(4-amp)PF₆ (6). This reaction used 4-amp, 0.21 mL (2.1 mmol), and AgPF₆, 0.512 g (2.03 mmol), to yield 0.631 g (1.75 mmol, 86%). Colorless needle shaped crystals (from water) formed. Anal. Calcd for C₆H₈N₂F₆PAG: C, 19.96; H, 2.23; N, 7.76. Found: C, 20.27; H, 2.02; N, 7.32. Characteristic IR peaks (cm⁻¹): 3356, 1618, 1595, 1562, 1468, 1433, 1366, 1233, 1130, 1069, 995, 831, 619, 557.

Physical Measurements. IR spectra (KBr disk) were recorded on a Jasco 5300 FT/IR infrared spectrometer. C, H, N analysis was performed on a Perkin-Elmer 240C elemental analyzer or a Perkin-Elmer 2400 CHNS/O analyzer. ¹H and ¹³C NMR spectra were recorded in CH₃CN-*d*₃ using a 200 MHz, Bruker AC200 model NMR spectrometer. Tetramethylsilane was used as internal standard.

X-ray Crystallography. X-ray data were collected for colorless crystals with dimensions 0.32 × 0.28 × 0.24 mm³ for **1**, 0.80 × 0.44 × 0.40 mm³ for **2**, 0.30 × 0.25 × 0.20 mm³ for **4**, 0.56 × 0.42 × 0.40 mm³ for **5**, and 0.40 × 0.35 × 0.35 mm³ for **6** on an Enraf Nonius CAD-4 diffractometer using graphite monochromated Mo Kα radiation. Absorption corrections based on ψ -scans¹² were applied. The structures were solved by a combination of heavy atom and direct methods (SHELXS-97) and refined (over *F*²) by least-squares techniques (SHELXL-97).¹³ Drawings were made using ORTEP-III¹⁴ and RasMol 2.6.¹⁵ Crystal data are presented in Table 1, and selected interatomic distances and angles are in Table 2. Powder diffractograms were measured using PW3710 model Philips Analytical X-ray diffractometer.

Results

Structure of Ag(2-amp)BF₄ (1). The Ag⁺ ion coordinates linearly with an amine nitrogen atom and a pyridine nitrogen atom from two different ligands. The resulting polymeric chain has one Ag(2-amp)BF₄ in the asymmetric unit (Figure 1). The polymeric repeat unit is Ag–amp–Ag', where the neighboring silver centers in the chain are related by a glide plane. The adjacent chains are connected by weak Ag...Ag contacts and π -stacking interactions (Figure 2). The anions are involved in hydrogen bonding with the amino group of the ligand, with H...F distances in the range 2.4–2.5 Å.

Structure of Ag₂(2-amp)₃(PF₆)₂ (2). The cation is monomeric and dinuclear and is very different from **1**. The asymmetric unit (Figure 3) consists of two chemically inequivalent 3-coordinate Ag(I) centers and two PF₆⁻ ions, one of which is disordered. There are three ligands in the asymmetric unit. Two of them are acting as chelates with

(11) (a) Withersby, M. A.; Blake, A. J.; Champness, N. R.; Hubberstey, P.; Li, W.-S.; Schröder, M. *Angew. Chem., Int. Ed. Engl.* **1997**, *36*, 2327. (b) Jung, O.-S.; Kim, Y. J.; Lee, Y.-A.; Chae, H. K.; Jang, H. G.; Hong, J. *Inorg. Chem.* **2001**, *40*, 2105. (c) Kang, Y.; Lee, S. S.; Park, K.-M.; Lee, S. H.; Kang, S. O.; Ko, J. *Inorg. Chem.* **2001**, *40*, 7027. (d) Tong, M.-L.; Chen, X.-M.; Ye, B.-H. *Inorg. Chem.* **1998**, *37*, 5278. (e) Hirsch, K. A.; Wilson, S. R.; Moore, J. S. *Inorg. Chem.* **1997**, *36*, 2960. (f) Perreault, D.; Drouin, M.; Michel, A.; Harvey, P. D. *Inorg. Chem.* **1992**, *31*, 3688. (g) Melcer, N. J.; Enright, G. D.; Ripmeester, J. A.; Shimizu, G. K. H. *Inorg. Chem.* **2001**, *40*, 4641.

(12) North, A. C. T.; Phillips, D. C.; Mathews, F. S. *Acta Crystallogr.* **1968**, *A24*, 351.

(13) Sheldrick, G. M. *SHELXS-97 and SHELXL-97*; University of Göttingen: Göttingen, Germany, 1997.

(14) Burnett, M. N.; Johnson, C. K. *ORTEP-III: Oak Ridge Thermal Ellipsoid Plot Program for Crystal Structure Illustrations*; Oak Ridge National Laboratory Report ORNL-6895; Oak Ridge National Laboratory: Oak Ridge, TN, 1996.

(15) Sayle, R.; Milner-White, E. J. *Trends Biochem. Sci.* **1995**, *20*, 374.

Table 1. Crystallographic Data for **1**, **2**, **4**, **5**, and **6**

	1	2	4	5	6
formula	C ₆ H ₈ Ag N ₂ BF ₄	C ₁₈ H ₂₄ Ag ₂ N ₆ F ₁₂ P ₂	C ₁₈ H ₂₄ Ag ₂ N ₆ F ₁₂ P ₂	C ₁₅ H _{20.50} Ag ₂ N _{5.50} B ₂ F ₈	C ₆ H ₈ AgN ₂ F ₆ P
fw	302.82	830.11	830.11	667.23	360.98
<i>a</i> (Å)	16.788(2)	10.029(7)	10.4482(7)	9.272(2)	5.2089(7)
<i>b</i> (Å)	11.5719(6)	20.291(12)	11.1468(9)	16.164(12)	14.3950(17)
<i>c</i> (Å)	11.3864(7)	13.907(6)	12.2720(11)	27.851(2)	7.0149(14)
α (deg)	90	90	81.018(7)	90	90
β (deg)	123.671(8)	95.38(5)	80.868(6)	90	96.538(14)
γ (deg)	90	90	80.977(6)	90	90
<i>V</i> (Å ³)	1840.9(3)	2818(3)	1380.99(19)	4174(3)	522.6(13)
<i>Z</i>	8	4	2	8	2
space group	<i>C2/c</i>	<i>P2₁/a</i>	<i>P1</i>	<i>C222₁</i>	<i>P2₁/m</i>
<i>T</i> (°C)	20	20	20	20	20
λ (Å)	0.71073	0.71073	0.71073	0.71073	0.71073
<i>D</i> _{calcd} (g cm ⁻³)	2.185	1.957	1.996	2.123	2.294
μ (cm ⁻¹)	22.10	16.04	16.36	19.62	21.40
<i>R</i> (<i>F</i> _o ²) ^a	0.0195	0.0581	0.0569	0.0766	0.0474
<i>R</i> _w (<i>F</i> _o ²) ^b	0.0478	0.1534	0.1608	0.2064	0.1241

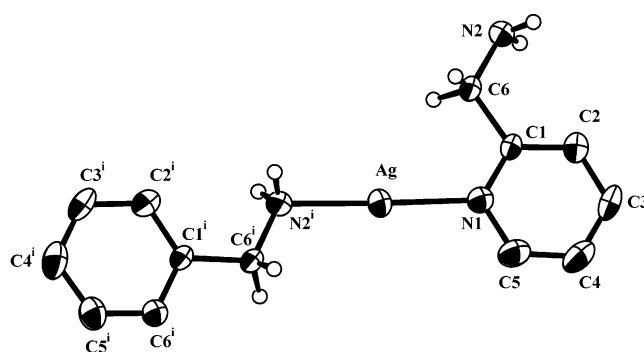
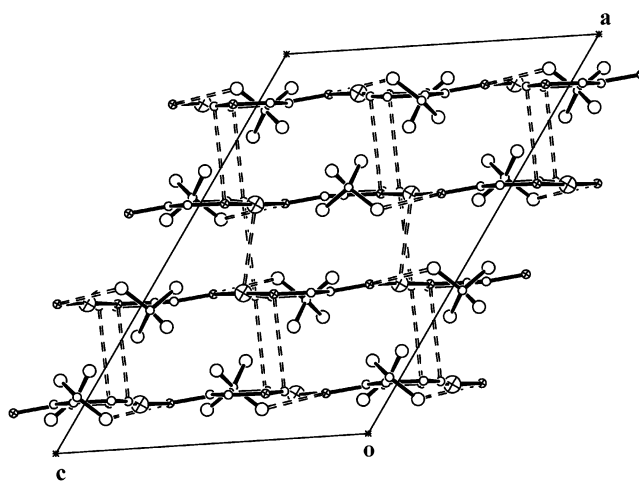
$$^a R = \sum ||F_o| - |F_c|| / \sum |F_o|. \quad ^b R_w = [\sum w(F_o^2 - F_c^2)^2 / \sum wF_o^4]^{1/2}.$$

Table 2. Selected Bond Lengths (Å) and Angles (deg) and Important Noncovalent Contacts for **1**, **2**, **4**, **5**, and **6**^a

Ag ₂ (2-amp)BF ₄ (1)			
Ag1–N1	2.1515(18)	Ag1–N2#1	2.1576(18)
N1–Ag1–N2#1	177.81(7)		
C5#4...C5#5	3.462(4)		
Ag1...Ag1#2	3.2510(6)		
Ag ₂ (2-amp) ₃ (PF ₆) ₂ (2)			
Ag1–N3	2.184(5)	Ag1–N2	2.284(7)
Ag1–N1	2.313(6)	Ag2–N4	2.193(7)
Ag2–N5	2.250(6)	Ag2–N6	2.401(7)
N3–Ag1–N2	147.7(2)	N3–Ag1–N1	138.2(2)
N2–Ag1–N1	73.7(2)	N4–Ag2–N5	151.1(2)
N4–Ag2–N6	135.1(3)	N5–Ag2–N6	73.6(2)
Ag1...Ag2	3.067(2)		
N1...C13	3.302(9)	N1...N5	3.510(8)
C1...C13	3.442(11)		
Ag ₂ (3-amp) ₃ (PF ₆) ₂ (4)			
Ag1–N1	2.271(5)	Ag1–N4#2	2.357(10)
Ag1–N6#1	2.255(5)	Ag2–N2	2.274(5)
Ag2–N3	2.277(4)	Ag2–N5	2.256(4)
N6#1–Ag1–N1	122.85(16)	N1–Ag1–N4#2	120.7(4)
N6#1–Ag1–N4#2	114.7(4)	N5–Ag2–N3	117.92(15)
N5–Ag2–N2	129.21(18)	N2–Ag2–N3	112.64(19)
C17#1...C4	3.530(10)	C17#1...C5	3.574(8)
C16#1...N1	3.572(7)	C15#1...N1	3.537(7)
Ag(4-amp)BF ₄ ·0.75CH ₃ CN (5)			
Ag1–N1	2.158(7)	Ag1–N2#1	2.162(7)
Ag2–N3	2.128(7)	Ag2–N4#3	2.154(9)
N1–Ag1–N2#1	175.0(4)	N3–Ag2–N4#3	176.9(4)
Ag1...Ag2	3.3699(15)		
Ag(4-amp)PF ₆ (6)			
Ag–N1	2.144(6)	Ag–N2#1	2.143(5)
N2#1–Ag–N1	174.84(16)		
N1#3...N2#1	3.379(7)	C3#3...N1	3.571(10)
C4#3...N1	3.421(8)	C2#4...N2#3	3.319(6)

^a Symmetry transformations used to generate equivalent atoms: (#1) *x*, *−y*, *z* + 1/2; (#2) *−x* + 1, *y*, *−z* + 1/2; (#4) *x*, *−y*, *z* + 3/2; (#5) *−x* + 1, *−y*, *−z* + 2 for **1**; (#1) *x* + 1, *y*, *z*; (#2) *x*, *y*, *z* + 1 for **4**; (#1) *x* + 1, *y*, *z*; (#3) *x* + 1/2, *y* − 1/2, *z* for **5**; (#1) *x* + 1, *y*, *z* − 1; (#3) *x* + 1, *y*, *z*; (#4) *x* + 1, *−y* + 3/2, *z* for **6**.

unsymmetrical Ag–N bonds. The third ligand bridges the two Ag(I) centers by coordinating through the amine (N4) and pyridine (N3) nitrogen atoms. The coordination around Ag1 is therefore, made up of two pyridine and one amine nitrogen atoms. Ag2, on the other hand, has coordination with one pyridine and two amine nitrogen atoms. The bridging ligand binds more strongly with the Ag⁺ ions with

**Figure 1.** ORTEP view of the cation in **1** with atom labeling. In this and later ORTEP drawings, atoms are represented as 50% probability ellipsoids, and ring hydrogens are omitted for clarity. Symmetry code: (i) *x*, *−y*, *z* + 1/2.**Figure 2.** Packing diagram of **1**. Large balls (i.e., circles with × markings) represent Ag atoms, and small balls, the N atoms. Intermolecular contacts (Ag...Ag, ring stacking, and hydrogen bonding) are indicated by broken lines.

equal Ag–N distances. Both Ag(I) centers have a distorted trigonal planar coordination. Ag1 and Ag2 deviate by 0.07 and 0.04 Å, respectively, from their corresponding coordination planes. The chelating angle around both the Ag atoms is acute. The short chelating angles along with unsymmetrical chelating Ag–N distances give a distorted “Y” shaped geometry around both the Ag centers. The unsymmetrical

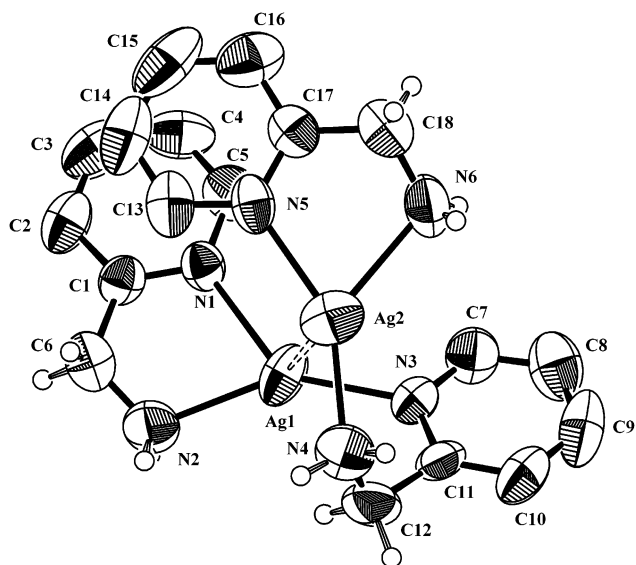


Figure 3. ORTEP view of the dinuclear cation in **2** with atom labeling.

nature of the chelation is more pronounced for Ag2 than Ag1, as can be seen from the Ag–N distances.

There is an intramolecular $\text{Ag}\cdots\text{Ag}$ interaction between the two Ag centers (Table 2). The $\text{Ag}\cdots\text{Ag}$ distance falls in the range observed in other discrete molecules: (i) 2.88 Å in dinuclear, 2-coordinate glycine silver(I) nitrate,¹⁶ (ii) 2.778 and 2.834 Å in dinuclear, 2-coordinate bis(3-hydroxy-4-phenyl-2,2,3-trimethylcyclohexane carboxylato)disilver(I) dihydrate,¹⁷ (iii) 3.38–3.49 Å in dinuclear, 3-coordinate silver(I)–tricyclohexylarsine adduct,¹⁸ (iv) 3.177 Å in hexanuclear, 2-coordinate Ag(I) imidazole perchlorate,¹⁹ (v) 3.085 Å in dinuclear, 2-coordinate $\text{Ag}_2(\text{dmp})_2(\text{NO}_3)_2$ ²⁰ (dmp = 2,9-dimethyl-1,10-phenanthroline), and (vi) 3.087 Å in dinuclear, 4-coordinate $\text{Ag}(\text{dmbp})\text{NO}_3$ ²¹ (dmbp = 6,6'-dimethyl-2,2'-bipyridine). The unit cell has four independent molecules in which the cationic and anionic units are arranged in alternate layers (Figure 4). The anions are involved in strong hydrogen bonding with the amine hydrogens, with $\text{H}\cdots\text{F}$ distances in the range 2.3–2.6 Å. There is no Ag–F interaction present.

Structure of $\text{Ag}_2(\text{3-amp})_3(\text{PF}_6)_2$ (4**).** There are two 3-coordinate Ag(I) centers in the asymmetric unit of **4** (Figure 5). All the three ligands in the asymmetric unit play a bridging role, connecting the silver centers. Ag1 is coordinated to one pyridine and two amine N atoms from three different ligands. There are two short and one long Ag–N bonds. The N–Ag–N angles are close to 120°, thus giving a trigonal planar geometry to Ag1. However, the Ag1 atom deviates from the plane defined by its coordinating N atoms by 0.18 Å. Coordination around Ag2 is completed by two

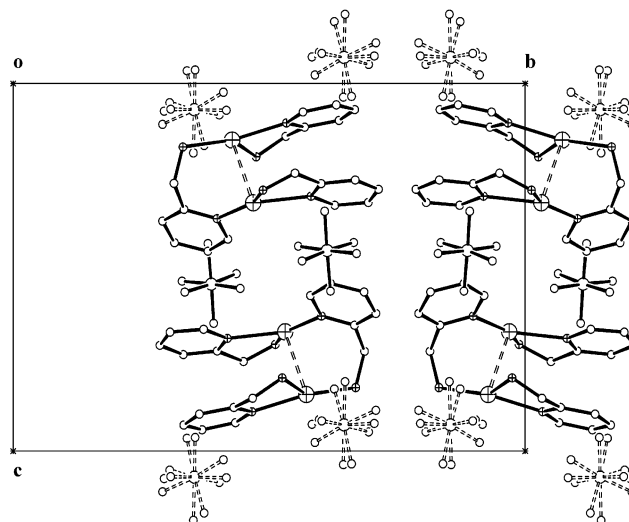


Figure 4. Packing diagram of **2**. Large balls represent Ag atoms, and small balls, N atoms. P atoms are shown as large open circles. Ring C and F atoms are shown as small open circles. $\text{Ag}\cdots\text{Ag}$ contacts and bonds from P to disordered F atoms are shown as broken lines.

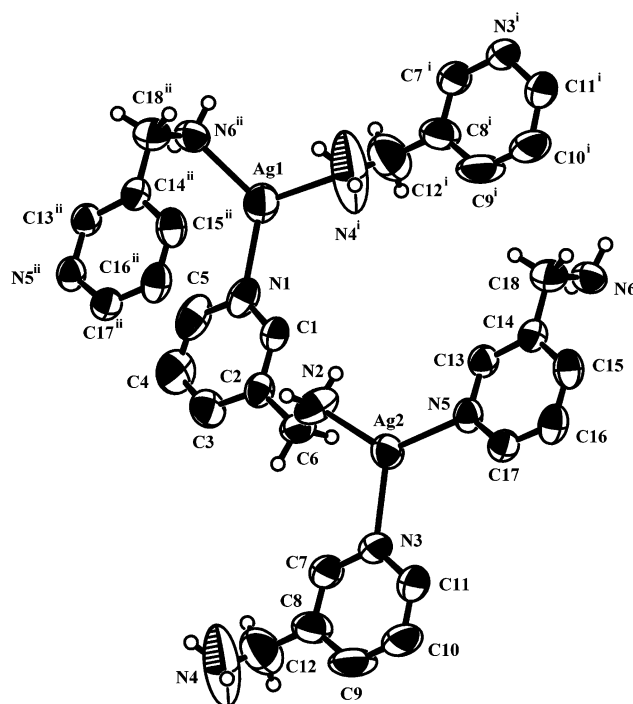


Figure 5. ORTEP view of the cation in **4** with atom labeling. Symmetry codes: (i) $x, y, z + 1$; (ii) $x + 1, y, z$.

pyridine and one amine nitrogen atom from three different ligands. There are one short Ag–N bond and two relatively longer Ag–N bonds. The asymmetry in the Ag2–N bond distances are much less when compared to Ag1–N distances. The Ag2 atom lies more closely to the plane defined by its coordinating N atoms (deviation, 0.06 Å). The angles around Ag2 are close to 120°, and hence, the geometry is trigonal planar. The amino nitrogens deviate greatly (N2, 0.98 Å; N4, 0.95 Å; N6, 1.41 Å) from the mean planes defined by their associated ring atoms.

The structure is a 2-D network. The anions, half of which are disordered, fit into the channels formed by the cationic

- (16) Mohana Rao, J. K.; Viswamitra, M. A. *Acta Crystallogr.* **1972**, B28, 1484.
 (17) Coggon, P.; McPhail, A. T. *J. Chem. Soc., Chem. Commun.* **1972**, 91.
 (18) BowmakerEffendy, G. A.; Junk, P. C.; White, A. H. *J. Chem. Soc., Dalton Trans.* **1998**, 2131.
 (19) Eastland, G. W.; Mazid, M. A.; Russell, D. R.; Symons, M. C. R. *J. Chem. Soc., Dalton Trans.* **1980**, 1682.
 (20) Swarnabala, G.; Rajasekharan, M. V. *Polyhedron* **1996**, 15, 3197.
 (21) Venkatalakshmi, N.; Rajasekharan, M. V.; Mathews, I. I. *Transition Met. Chem.* **1992**, 17, 455.

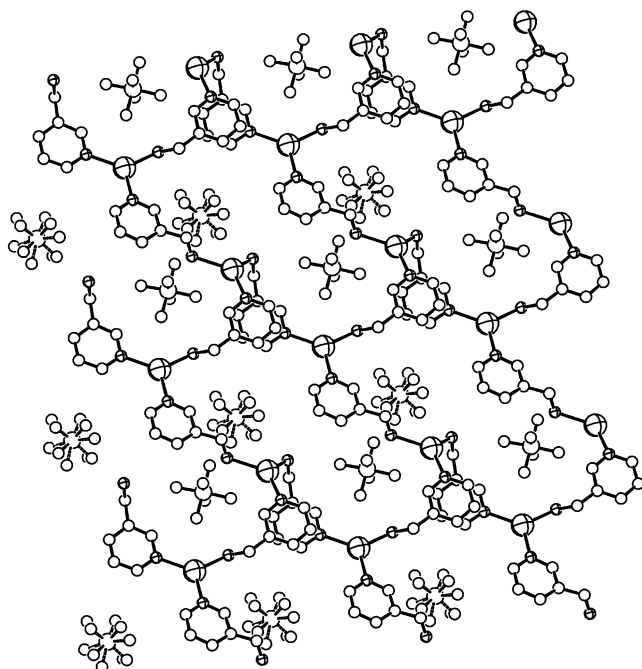


Figure 6. Packing diagram of **4**. Ag atoms are shown as large balls. N atoms are represented as small balls, P atoms as large open circles, and F atoms and ring C atoms as small open circles. The bonds from P to disordered F atoms are shown as broken lines.

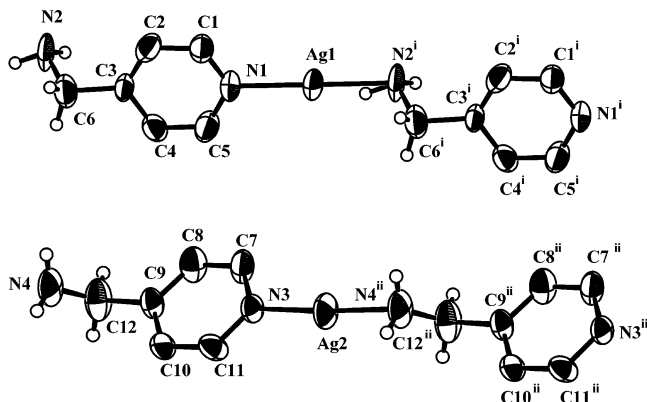


Figure 7. ORTEP view of the cations in **5** with atom labeling. Symmetry codes: (i) $x + 1, y, z$; (ii) $x + 1/2, y - 1/2, z$.

units (Figure 6). They are involved in strong hydrogen bonding with the amino groups, with the $\text{H}\cdots\text{F}$ distances in the range 2.2–2.6 Å. No $\text{Ag}\cdots\text{Ag}$ contacts are observed, but stacking is present.

Structure of $\text{Ag}(4\text{-amp})\text{BF}_4 \cdot 0.75\text{CH}_3\text{CN}$ (5**).** The asymmetric unit is made up of two $\text{Ag}(4\text{-amp})^+$ moieties (Figure 7), two anions, one of which is disordered, and CH_3CN solvent molecules with partial site occupation. Ag1 and Ag2 are coordinated to a pyridine and an amine N atom from two different ligands, with a linear geometry. The geometry around Ag2 is more linear than that around Ag1. The Ag1–N distances are equal, while Ag2 has significantly different Ag–N distances.

The unit cell has two different types of polymer chains (Figure 8). There are 8 chains corresponding to the symmetry positions of the space group. The repeat unit of this chain is one $(\text{Ag}1\text{-amp})^+$. The second type of chain is built out of

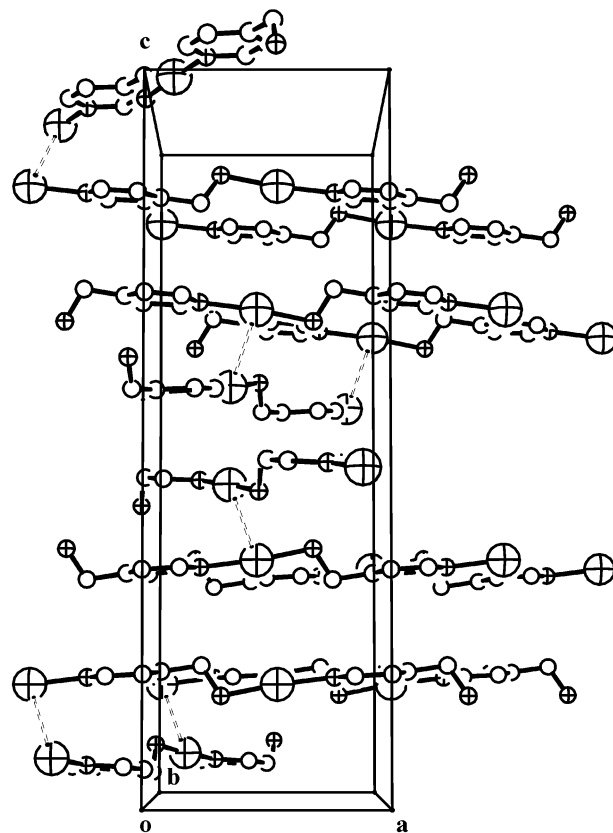


Figure 8. Packing of 12 symmetry related chains in **5**. Broken lines represent the $\text{Ag}\cdots\text{Ag}$ interactions. Ag atoms are shown as large balls, and N atoms, as small balls. C atoms are shown as small open circles.

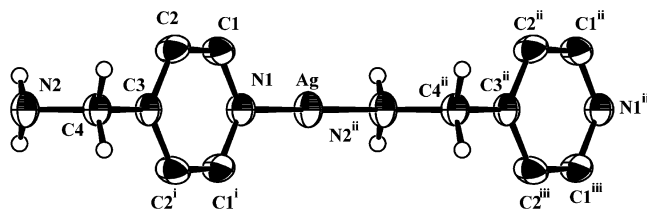


Figure 9. ORTEP view of the cation in **6** with atom labeling. Symmetry codes: (i) $x, -y + 3/2, z$; (ii) $x + 1, y, z - 1$; (iii) $x + 1, -y + 3/2, z - 1$.

$(\text{Ag}2\text{-amp-Ag}2\text{-amp})^{2+}$ repeat units. In this repeat unit, the two silver centers are related by the C -centering operation. Because of the symmetry relation, this type of chains are only 4 in number. Altogether, there are 12 chains in the unit cell. The anions sit within the cationic layers and strongly hydrogen bond to the amino groups, with $\text{H}\cdots\text{F}$ distances in the range 2.0–2.4 Å. The two types of silver atoms, Ag1 and Ag2, are separated by 3.370(2) Å, indicating the presence of a weak $\text{Ag}\cdots\text{Ag}$ interaction. The structural features of **5** are similar to that of $\text{Ag}(4\text{-amp})\text{ClO}_4$,² except that the perchlorate salt crystallizes in a hexagonal space group and all the 12 chains are identical.

Structure of $\text{Ag}(4\text{-amp})\text{PF}_6$ (6**).** This is the simplest of all the structures discussed. The asymmetric unit has one $\text{Ag}(4\text{-amp})\text{PF}_6$ (Figure 9). The polymer repeat unit is $\text{Ag}(4\text{-amp})^+$, which is situated on a mirror plane. The 2-coordination around Ag is completed by the coordination of a pyridine N and an amine N atom from two translationally related ligands. The geometry around Ag is nearly linear.

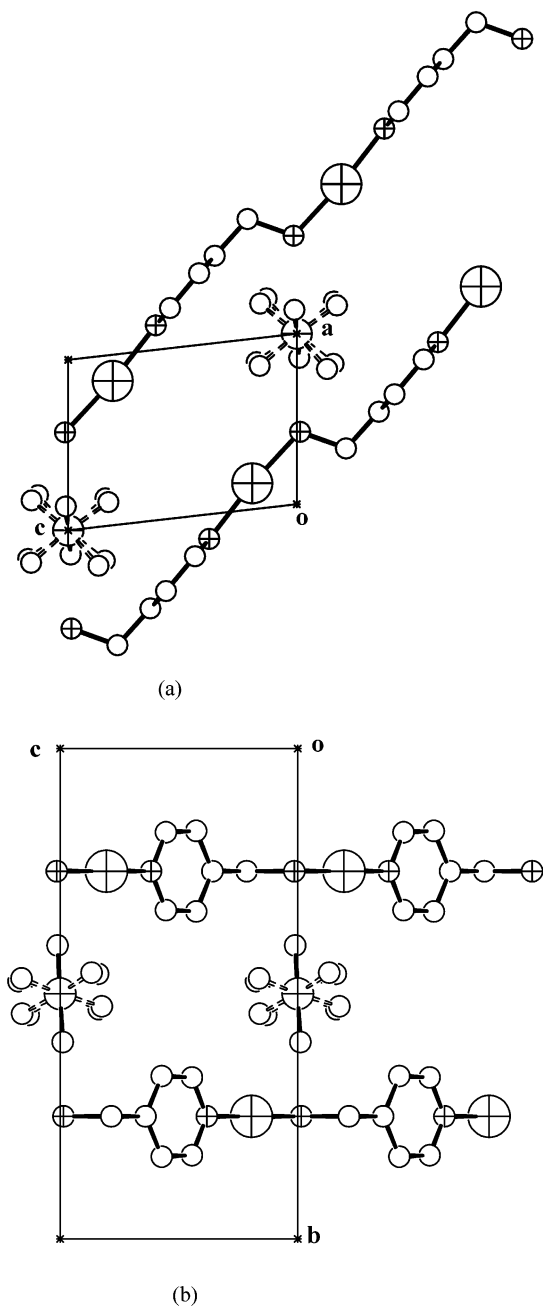


Figure 10. Two views showing the packing of cationic chains and anions in the unit cell of **9**: (a) *ac*-plane, (b) *bc*-plane. Ag atoms are shown as large balls, P atoms as medium balls, and N atoms as small balls. C atoms and F atoms are shown as open circles. The bonds from P to disordered F atoms are shown as broken lines.

There are two polymeric chains in the unit cell. The cationic chains and the anions, which are disordered, are arranged in alternate layers (Figure 10). The anions are involved in hydrogen bonding with the amino groups, with $\text{H}\cdots\text{F}$ distances in the range 2.2–2.3 Å. Ring stacking is observed. However, there is no $\text{Ag}\cdots\text{Ag}$ interaction.

Discussion

Synthesis. In all cases, except **2** and **4**, the initial precipitate formed when the ligand and Ag(I) salts are mixed is the same as the crystals obtained by recrystallization of this precipitate from water. This fact is proved by the

Scheme 1. Torsion Angles^a

	2-amp	3-amp	4-amp
NO_3^- ^a	180	-	-
ClO_4^- ^b	-170, -168	-158, 145	-112
BF_4^-	170	-	-68, 109
PF_6^-	23, -30, 80	-51, 111, 90	-90

^a Reported in units of degrees. These are defined for the atom sequence 1, 2, 3, 4 and follow the standard convention of ref 49. *a* indicates ref 27; *b* indicates ref 2.

agreement of the IR of the precipitate and the single crystals. Also, the experimental powder pattern of the precipitate and the powder pattern calculated on the basis of the crystal structure²² are the same. However, in the case of **2** and **4** there are differences in the IR of the precipitate and the crystals as well as the X-ray powder patterns of the precipitate and the calculated powder pattern. The C, H, N analyses of the precipitate formed in these two cases clearly show that they are 1:1 complexes. Slow recrystallization from water leads to reorganization to 2:3 compounds. It is to be noted that both the initial preparation and the recrystallization result in (near) quantitative yields and both samples are analytically pure.

Ligand and Anion Control on Structure Formation.

The two main factors that control the structure formed in all the complexes discussed are the conformational flexibility of the ligand and role of anion in influencing the structure packing.

Unlike ligands such as pyrazine, where there is no flexibility in the ligand, the amp ligands have a flexible $\text{CH}_2\text{-NH}_2$ group in which the torsion about the $\text{C}(\text{ring})\text{-C}(\text{methylene})$ bond may vary in the range 0–180°. Further, in the case of 2-amp, depending on the torsion angles, the ligand can bind in either the bridging or the chelating mode. Both these modes have been noted previously.^{23–26} The torsion angles observed for the various structures are given in Scheme 1.

The variation in the anion size and shape has a marked influence on the crystal packing. The van der Waals radii of BF_4^- and ClO_4^- are nearly same (2.78 Å) while that of PF_6^- is much larger (2.98 Å). The PF_6^- salts show greatest deviation in the present series of structures. In the case of 2-amp, it results in a chelated dinuclear complex, while in the case of 3-amp, it forms a planar 3-connected network. On the other hand, in the case of 4-amp, the planar network

(22) Kraus, W.; Nolze, G. *Powder Cell for Windows version 2.3*; Federal Institute for Materials Research and Testing: Berlin, Germany, 1999.

(23) Michelsen, K. *Acta Chem. Scand.* **1970**, *24*, 2003.

(24) Hodgson, D. J.; Michelsen, K.; Pedersen, E. *Acta Chem. Scand.* **1990**, *44*, 1002.

(25) Katz, B. A.; Strouse, C. E. *Inorg. Chem.* **1980**, *19*, 658.

(26) Mikami-Kido, M.; Saito, Y. *Acta Crystallogr.* **1982**, *B38*, 452.

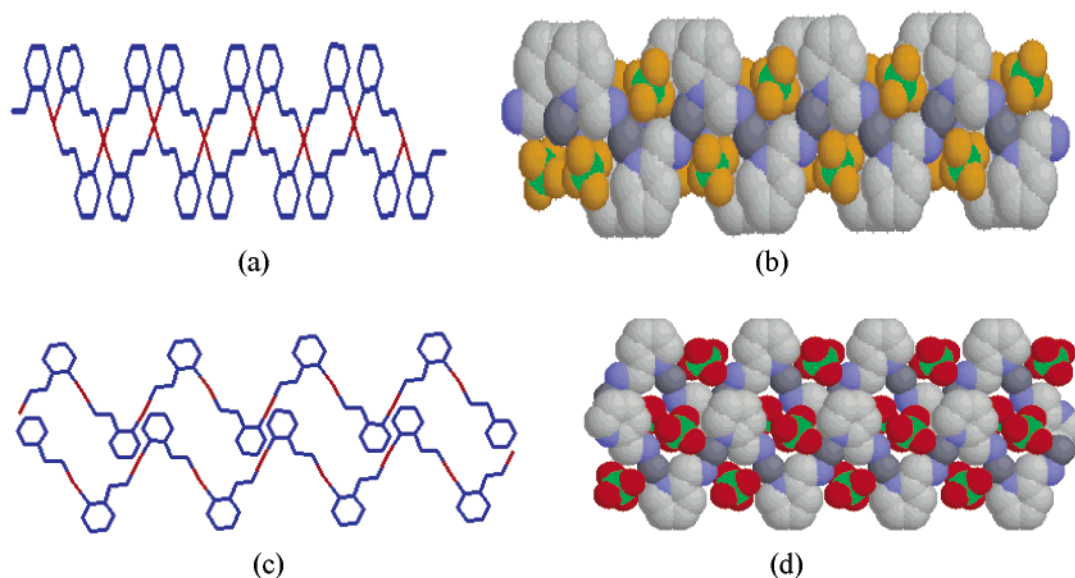


Figure 11. Stick representations showing the channels and space filling models showing packing of anions in Ag(2-amp)BF₄ (a and b). The packing of the ClO₄⁻ analogue is shown for comparison (c and d, redrawn on the basis of data in ref 2).

formed by Ag⁺⋯Ag bonds in BF₄⁻ and ClO₄⁻ salts is broken to form a simple chain structure in the PF₆⁻ salt.

Comparisons among the Ag(2-amp)X Chain Systems. The chains of Ag(2-amp)NO₃,²⁷ Ag(2-amp)ClO₄,² and Ag(2-amp)BF₄ (**1**) have a wavelike appearance (Figure 11). In all the three cases, the centrosymmetrically related chains have a phase difference. Besides the phase difference, chains of Ag(2-amp)NO₃ and Ag(2-amp)ClO₄ also have a lateral displacement, which generates voids large enough to accommodate the anions. The weak Ag⁺⋯Ag interactions present in **1** prevent the lateral displacement of adjacent chains, and therefore, the anions sit along the chain edges instead of being filled in the cavities.

Ag₂(2-amp)₃(PF₆)₂: A Helicate Held by Ag⁺⋯Ag Interaction. The fact that chelation is possible in 2-amp is seen in the structure of **2**, which is zero-dimensional having a dinuclear cation with 3-coordinate Ag atoms. Though many of the previously reported 3-coordinate Ag(I) compounds are polymeric,^{28–37,40,41} discrete systems are also known.^{18,21,38,39} Ag₂(2-amp)₃²⁺ has a helicate conformation (Figure 3) which is held by Ag⁺⋯Ag interaction. A remarkable feature of this conformation is that the two pyridyl rings are almost fully

eclipsed (N1–Ag1–Ag2–N5 torsion = 2.90°). Such a stacking of pyridyl rings is expected to cause a repulsive interaction. Apparently to reduce this repulsion, the structure tends to open up slightly as one moves from the center of the helicate toward the pyridyl rings (Ag1⋯Ag2 = 3.07 Å, N1⋯N5 = 3.51 Å, angle between the two pyridyl ring mean planes = 12°). Upon examining molecular models, it is seen that the other possible conformation of the helicate will have even greater repulsion due to NH₂⋯ring interaction. It is therefore clear that the helicate structure is stabilized by an attractive Ag⁺⋯Ag interaction. Another contributing factor is the packing of the cations and anions of similar size in alternate layers in the crystal.

Ag(I) complexes are generally very labile in solution, and the helicate structure may not be retained in solution. ¹H and ¹³C NMR spectra in CH₃CN-*d*₃ do not distinguish between the three chemically inequivalent ligands.

Ag₂(3-amp)₃(PF₆)₂: 2-D Network of 3-Coordinate Ag(I). Compound **4** shows a network structure as is usually observed in other 3-coordinate Ag(I) systems. There are examples of triconnected silver(I) giving rise to either 2-D^{28–30,37,41} or 3-D^{30–32,34,40,41} network or framework structures. Among the 2-D networks, Ag₂(pyz)₃(BF₄)₂²⁸ shows a 2-D sheet structure, and Ag(TCB)CF₃SO₃³⁰ shows a honeycomb type layer arrangement which is homeotypic with CaCuP structure (pyz = pyrazine, TCB = 1,3,5-tricyanobenzene). The geometry of Ag1 and Ag2 is more planar in the present case, than in Ag₂(pyz)₃(BF₄)₂ or Ag(TCB)CF₃SO₃. The unsymmetrical Ag–N distances are comparable to those observed in the preceding examples.

(27) Swarnabala, G.; Rajasekharan, M. V. *Polyhedron* **1997**, *16*, 921.

(28) Carlucci, L.; Ciani, G.; Proserpio, D. M.; Sironi, A. *J. Am. Chem. Soc.* **1995**, *117*, 4562.

(29) Venkataraman, D.; Gardner, G. B.; Lee, S.; Moore, J. S. *J. Am. Chem. Soc.* **1995**, *117*, 11600.

(30) Gardner, G. B.; Venkataraman, D.; Moore, J. S.; Lee, S. *Nature* **1995**, *374*, 792.

(31) Aakeröy, C. B.; Beatty, A. M.; Helfrich, B. A. *J. Chem. Soc., Dalton Trans.* **1998**, 1943.

(32) Carlucci, L.; Ciani, G.; Proserpio, D. M.; Sironi, A. *Inorg. Chem.* **1997**, *36*, 1736.

(33) Hirsch, K. A.; Wilson, S. R.; Moore, J. S. *J. Am. Chem. Soc.* **1997**, *119*, 10401.

(34) Carlucci, L.; Ciani, G.; Proserpio, D. M.; Sironi, A. *Chem. Commun.* **1996**, 1393.

(35) Kuang, S.-M.; Zhang, Z.-Z.; Wang, Q.-G.; Mak, T. C. W. *Chem. Commun.* **1998**, 581.

(36) Smith, G.; Sagatys, D. S.; Campbell, C. A.; Lynch, D. E.; Kennard, C. H. L. *Aust. J. Chem.* **1990**, *43*, 1707.

(37) Sagatys, D. S.; Bott, R. C.; Smith, G. *Polyhedron* **1992**, *11*, 49.

(38) Lancashire, R. J. *Comprehensive Coordination Chemistry*; Wilkinson, G., Gillard, R. D., McCleverty, J. A., Ed.; Pergamon Press: Oxford, 1987; Vol. 5, p 784.

(39) Damayanthi, Y. M. Philos. Dissertation; University of Hyderabad, Hyderabad, India, 1991.

(40) Soma, T.; Yuge, H.; Iwamoto, T. *Angew. Chem., Int. Ed. Engl.* **1994**, *33*, 1665.

(41) Bu, W.-M.; Ye, L.; Fan, Y.-G. *Inorg. Chem. Commun.* **2000**, *3*, 194.

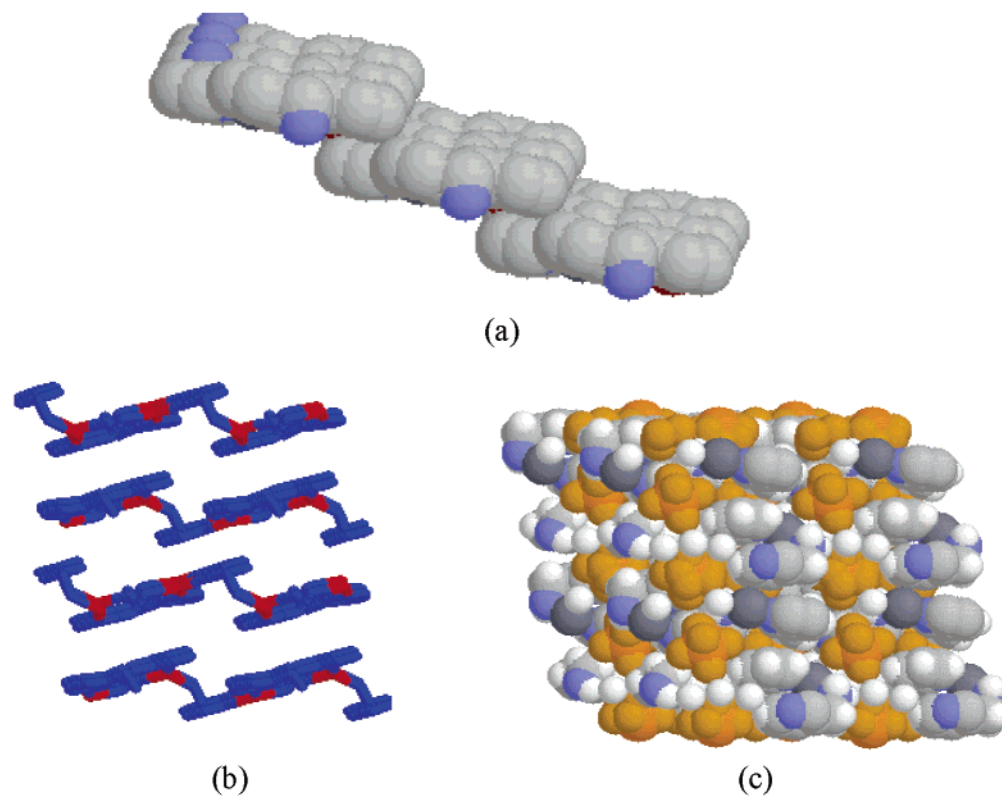


Figure 12. (a) Space filling model showing the terraced appearance of a single layer in **4**. (b) Stick representation showing channels between the layers. (c) Space filling model showing the ordered and disordered anions sitting in the channels in **4**.

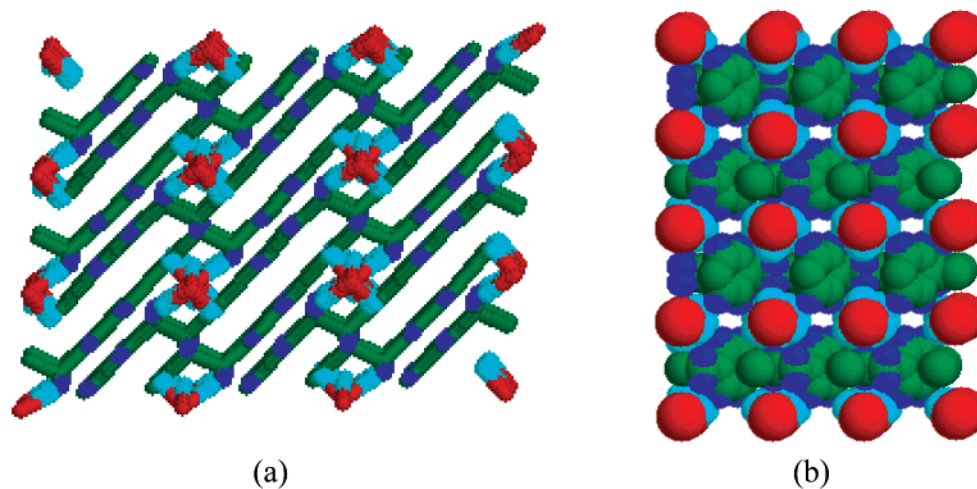


Figure 13. (a) Stick representation of the packing of cationic chains and anions in the unit cell. (b) Space filling model showing microchannels in **6**.

The layers in the 3-connected 2-D network have a terraced appearance as shown in Figure 12. The packing of layers generates channels which are occupied by the anions. The network structure is analogous to the 3-connected hexagonal plane nets formed by elements of the V group. The structure of certain binary compounds A_2X_3 , for example, As_2S_3 ,⁴² also has the same topology. The present network may be represented as ABX_3 where $A = Ag1$, $B = Ag2$, and $X = 3\text{-amp}$. The network generates large channels ($3 \times 6 \text{ \AA}^2$) big enough to accommodate the PF_6^- ions.

(42) Wells, A. F. *Structural Inorganic Chemistry*, 4th ed.; Oxford University Press: London, 1979; p 723.

Ag(4-amp)X: Anion Control of Packing Symmetry. The primary polymeric form in both BF_4^- and PF_6^- salts as well as the previously reported² ClO_4^- analogue is a saw-tooth-type one-dimensional chain. The simplest packing of the chains is observed in the PF_6^- salt. A groove is formed next to the “ CH_2 bends” of adjacent chains. The anions are accommodated in the grooves (Figure 13a). The space filling model shows that this packing leaves narrow ($2 \times 2 \text{ \AA}^2$) unoccupied microchannels (Figure 13b). There are no solvents or $Ag \cdots Ag$ bonds in this structure.

The packing in ClO_4^- and BF_4^- salts is closely related. Both structures contain $Ag \cdots Ag$ bonds which organize the

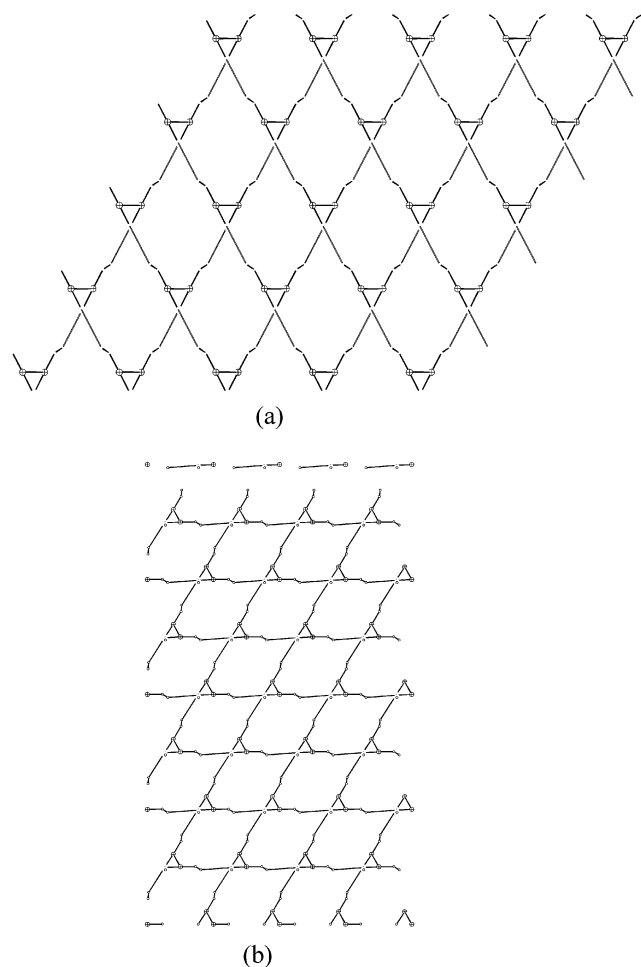


Figure 14. View showing 2-D networks in (a) $\text{Ag}(4\text{-amp})\text{ClO}_4 \cdot 0.5\text{H}_2\text{O}$ (drawn on the basis of data in ref 2) and (b) $\text{Ag}(4\text{-amp})\text{BF}_4 \cdot 0.75\text{CH}_3\text{CN}$. Some of the ring C atoms have been omitted for clarity.

chains into 3-connected 2-D networks (Figure 14). In the ClO_4^- salt, each layer is rotated by 60° with respect to its adjacent layer. Six such layers alternating with anion layers make up one unit cell. In the BF_4^- salt, there are only four layers, and there is no rotation between adjacent layers. The b -axis length of the orthorhombic cell is approximately $\sqrt{3}$ times the a -axis length. This cell therefore results from a distortion of the hexagonal cell toward lower symmetry. The orthorhombic packing results from flattening the hexagonal packing by about 33% and spreading it in the ab -plane along with a rotation of adjacent chains to correspond to orthorhombic symmetry.

Nature of $\text{Ag}\cdots\text{Ag}$ Interaction. Several recent papers have addressed the problem of $\text{Ag}\cdots\text{Ag}$ (as well as $\text{Cu}\cdots\text{Cu}$ and $\text{Au}\cdots\text{Au}$) interaction.⁴³ Arguments have been presented for and against an attractive $\text{Ag}\cdots\text{Ag}$ interaction. Controversy

arises mainly because, in a large number of such cases, there are ligands holding the Ag atoms close to each other in a rigid bridged conformation. Early theoretical attempts to understand closed shell metal–metal interactions were based on the extended Hückel molecular orbital (EHMO) method. Mehrotra and Hoffmann⁴⁴ concluded that 6s and 6p participation leads to the $d^{10}\text{--}d^{10}$ bonding interaction in Pt(0) compounds. Cotton et al.^{43b} ruled out a $\text{Ag}\cdots\text{Ag}$ bonding interaction using SCF- $X\alpha$ -SW molecular orbital calculations. They conclude that 5s and 5p orbitals are involved in M–L bonding, but not in $\text{Ag}\cdots\text{Ag}$ bonding. On the other hand, experimental evidence for a weak $\text{Ag}\cdots\text{Ag}$ bond is available from Raman bands associated with $\text{Ag}\cdots\text{Ag}$ stretching.⁴⁵ Ab initio calculations probing the nature of $d^{10}\text{--}d^{10}$ interactions have been reported for small model complexes of all three coinage metals.^{43c–h} The importance of eliminating the basis set superposition error which was present to varying extents in previous calculations has been recently emphasized by Hermann et al.^{43h} The main conclusions from the theoretical studies may be summarized as follows: (i) EHMO calculations generally produce an attraction due to the mixing of higher s and p orbitals with the d orbitals.⁴⁶ (ii) There is no bonding at the Hartree–Fock level. (iii) Attractive interaction arises in all three cases due to electron correlation, which is complemented in the case of gold by the relativistic effect. (iv) The $\text{Au}\cdots\text{Au}$ interaction tends to increase when Au is bound to soft ligands.^{43c} (v) The $\text{Au}\cdots\text{Au}$ interaction energy shows an R^{-6} dependence at long distances proving its dispersive (i.e., van der Waals type) character.^{43d} (vi) At shorter distances, the correlation energy includes both a dispersive and an ionic component.^{43g} (vii) The $\text{Cu}\cdots\text{Cu}$ interaction is about 2–3 times weaker than the $\text{Au}\cdots\text{Au}$ interaction,^{43c,h} while the $\text{Ag}\cdots\text{Ag}$ interaction is only about 15% weaker.^{43c} The minimum in the potential for all the three metals occurs at nearly the same internuclear separation (3.208–3.137 Å).^{43c}

The structure of **2** reported here is unique in the sense that it has a singly bridged structure⁴⁷ in which a potentially repulsive pyridyl–pyridyl interaction is avoided by distorting the helicate structure, but retaining the “ $\text{Ag}\cdots\text{Ag}$ bond”. It may be also mentioned that the interacting Ag centers in **2** have nonidentical coordination spheres. In order to see whether the $\text{Ag}\cdots\text{Ag}$ interaction in this ion can be modeled by the EH method, we performed an EHMO calculation at the experimental geometry.⁴⁸ The Ag–Ag reduced overlap population (ROP) obtained from this calculation is 0.048. In comparison, the Ag–N ROP ranges from 0.035 (for Ag–amino) to 0.150 (for Ag–pyridyl). This by itself indicates significant $\text{Ag}\cdots\text{Ag}$ bonding interaction. However, in the

(43) (a) Pyykkö, P. *Chem. Rev.* **1997**, *97*, 597. (b) Cotton, F. A.; Feng, X.; Matusz, M.; Poli, R. *J. Am. Chem. Soc.* **1988**, *110*, 7077. (c) Pyykkö, P.; Runeberg, N.; Mendizabal, F. *Chem. Eur. J.* **1997**, *3*, 1451. (d) Pyykkö, P.; Mendizabal, F. *Chem. Eur. J.* **1997**, *3*, 1451. (e) Fernández, E.; Lopez-de-Luzuriaga, J. M.; Monge, M.; Rodríguez, M. A.; Crespo, O.; Gimeno, M. C.; Laguna, A.; Jones, P. G. *Inorg. Chem.* **1998**, *37*, 6002. (f) El-Bahraoui, J.; Molina, J. M.; Olea, D. P. *J. Phys. Chem. A* **1998**, *102*, 2443. (g) Runeberg, N.; Schütz, M.; Werner, H.-J. *J. Chem. Phys.* **1999**, *110*, 7210. (h) Hermann, H. L.; Boche, G.; Schwerdtfeger, P. *Chem. Eur. J.* **2001**, *7*, 5333.

(44) Mehrotra, P. K.; Hoffmann, R. *Inorg. Chem.* **1978**, *17*, 2187.

(45) Perreault, D.; Drouin, M.; Machel, A.; Miskowski, V. M.; Schaefer, W.; Harvery, P. D. *Inorg. Chem.* **1992**, *31*, 695.

(46) For a tabulation of the EHMO work on copper and gold compounds, see ref 43a.

(47) For a singly bridged gold(I) structure with $\text{Au}\cdots\text{Au}$ interaction, see: Schmidbaur, H.; Graf, W.; Müller, G. *Angew. Chem., Int. Ed. Engl.* **1988**, *27*, 417.

(48) CACAO program: Mealli, C.; Proserpio, D. M. *J. Chem. Educ.* **1990**, *67*, 399. Neutral atom parameters for Ag were taken from: Glaus, S.; Calzaferrri, G. *J. Phys. Chem. B* **1999**, *103*, 5622.

(49) Allen, F. H.; Rogers, D. *Acta Crystallogr.* **1969**, *B25*, 1326.

light of the preceding discussion, which shows that the $d^{10}-d^{10}$ interaction is essentially of the dispersion type without involving any overlap, the EHMO result is not easy to explain. In other words, the ab initio methods (including electron correlation) as well as the EHMO method lead to $d^{10}-d^{10}$ attraction, but not for the same physical reason.

Conclusion

The structure of the BF_4^- salts of the Ag(I) polymers are grossly similar to those of the previously reported ClO_4^- salts. The PF_6^- anion, on the other hand, leads to very different structures. While the size of the anions and the preference of both BF_4^- and PF_6^- to hydrogen bond (with the NH_2 group) rather than to coordinate with Ag are responsible for the gross structural features, the finer details

are influenced by the $\text{Ag}\cdots\text{Ag}$ interaction. The decisive role of the latter closed shell interaction is most evident in the remarkable helicate structure of $\text{Ag}_2(2\text{-amp})_3(\text{PF}_6)_2$ and the $\text{Ag}\cdots\text{Ag}$ bonded chiral networks seen in $\text{Ag}(4\text{-amp})\text{X}$ ($\text{X} = \text{ClO}_4^-, \text{BF}_4^-$).

Acknowledgment. The X-ray data were collected at the diffractometer facilities at Hyderabad and Mumbai, established by the Department of Science and Technology, Government of India. This work was supported by CSIR, India.

Supporting Information Available: Crystallographic file, in CIF format. This material is available free of charge via the Internet at <http://pubs.acs.org>.

IC0342292